Supporting Information

for

Conformational Sensitivity of Surface Selection Rules for Quantitative Raman Identification of Small Molecules in Biofluid

Lei Li,[a] Chao Wang,[d] Lina Yang,[a] Mengke Su,[a] Fanfan Yu,[a] Li Tian,[a] and Honglin Liu*[a,b,c]

[a] College of Food Science and Engineering, Hefei University of Technology, Hefei, Anhui 230009, China.

[b] Engineering Research Center of Bio-process, Ministry of Education, China.

[c] Molecular Science and Biomedicine Laboratory, State Key Laboratory of Chemo/Bio-Sensing and Chemometrics, College of Chemistry and Chemical Engineering, College of Life Sciences, and Aptamer Engineering Center of Hunan Province, Hunan University, Changsha, Hunan 410082, China

[d] Key Laboratory of Neutronics and Radiation Safety, Institute of Nuclear Energy Safety Technology, Chinese Academy of Sciences, Hefei, Anhui 230031, China.

*Correspondence: liuhonglin@mail.ustc.edu.cn

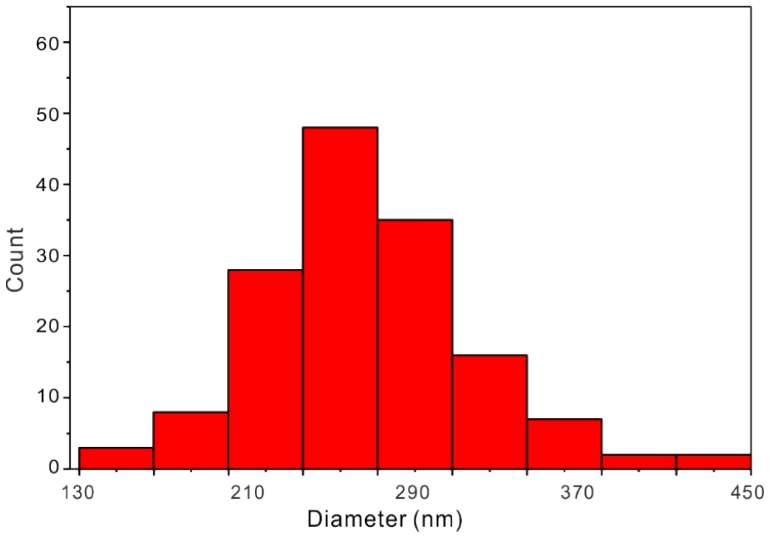

Figure S1. Diameter statistics of PS beads in Figure 1a.

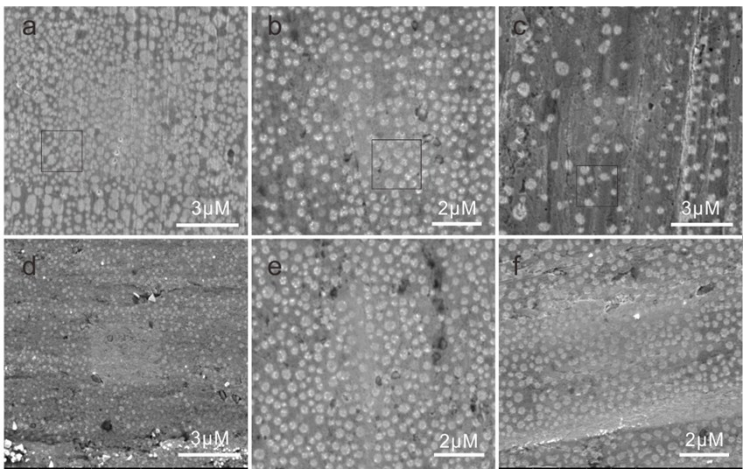

Figure S2. SEM images of polymer films formed under different experimental parameters. (a) PS/PMMA=1:9. (b) PS/PMMA=2:8. (c) PS/PMMA=3:7. Spin-coating speed at (d) 3500rpm, (e) 4000rpm and (f) 4500rpm.

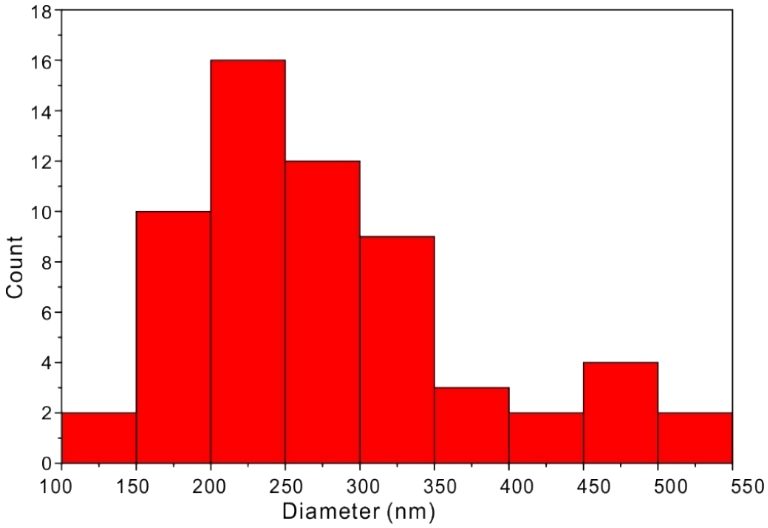

Figure S3. Diameter statistics of PS beads in Figure S2c.

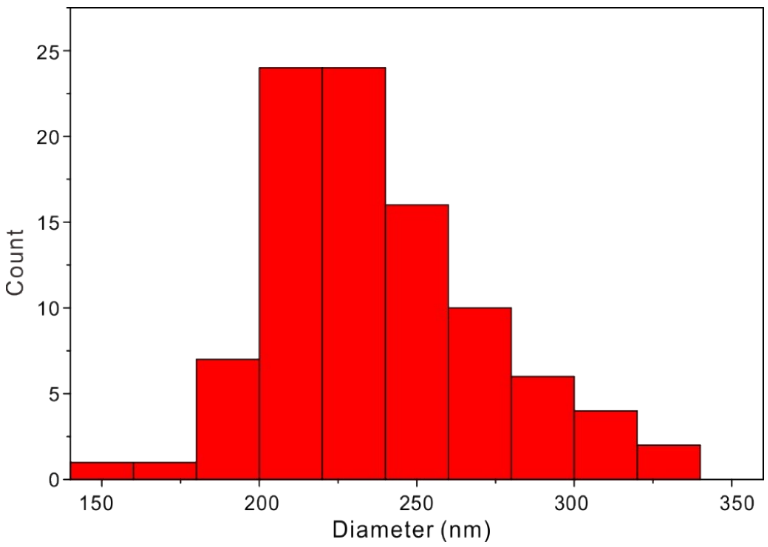

Figure S4. Diameter chart of the distribution holes in the PMMA film in Figure 1b.

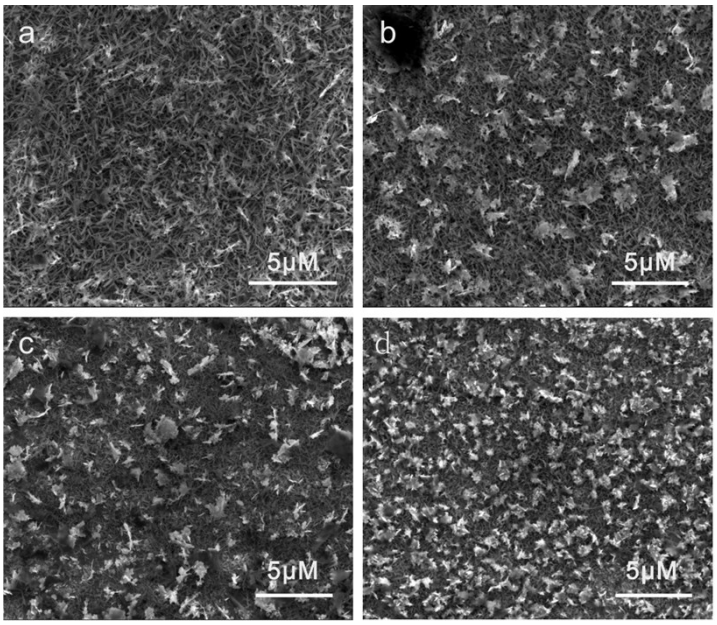

Figure S5. Ag structural growth conditions optimization with different soaking time in 3 mM $AgNO_3$ solution: (a) 5 s, (b) 10 s, (c) 15 s, (d) 2 mM $AgNO_3$ for 20s.

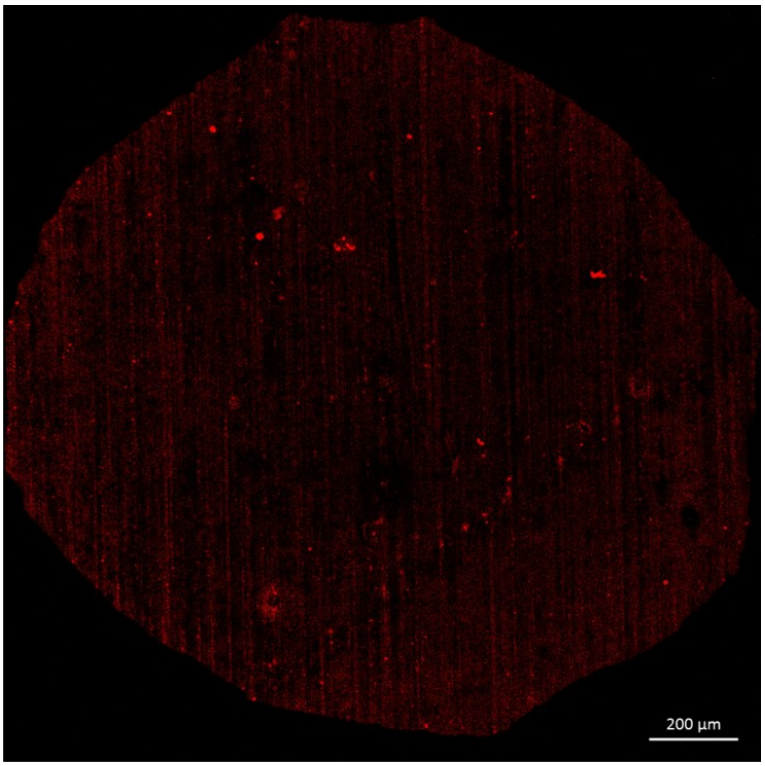

Figure S6. Confocal images of evaporation traces of R6G solution.

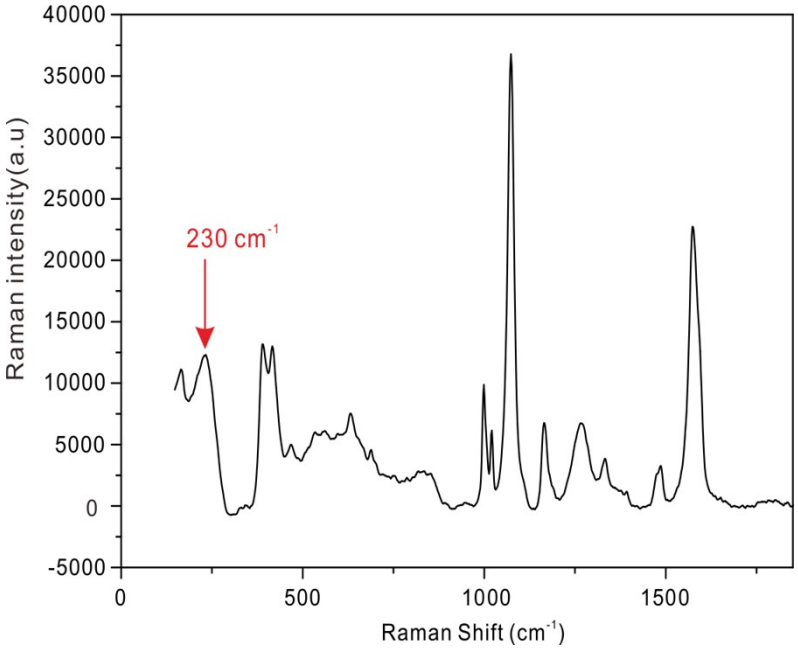

Figure S7. The Raman shift at 230 cm^{-1} represents the Ag-S bond.

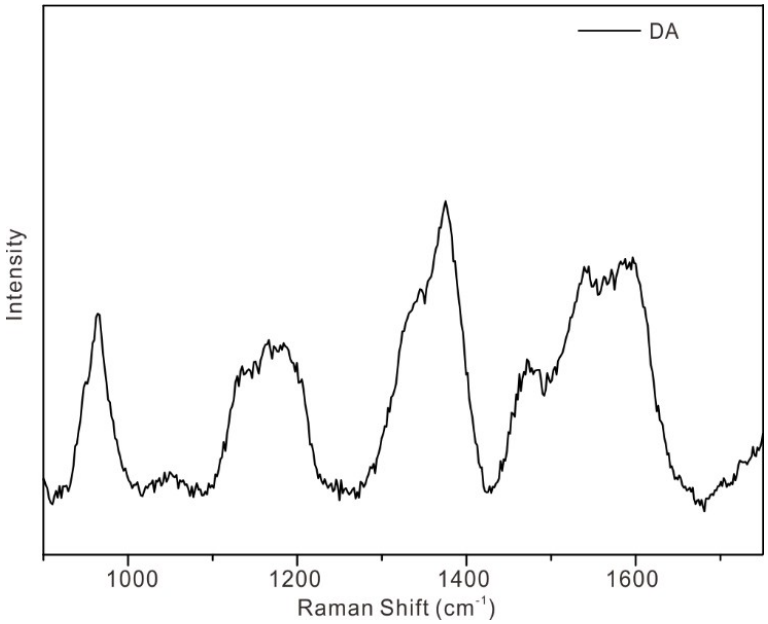

Figure S8. SERS signal of 10^{-4} M DA solution on superhydrophobic substrate.

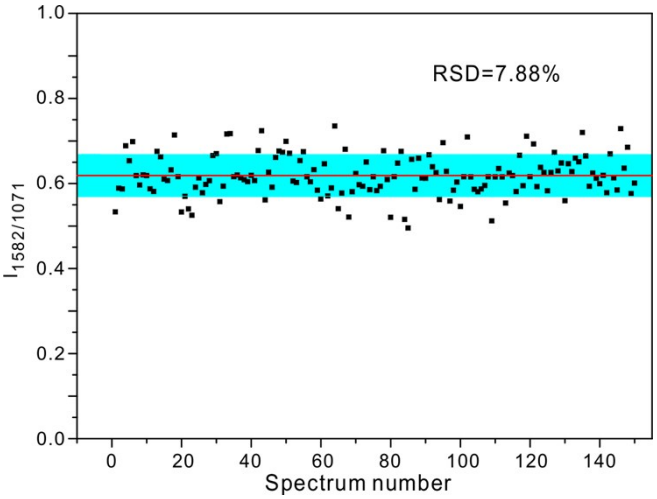

Figure S9. SERS reproducibility of MPBA on as-prepared platform via statistics analysis of a ratiometric indicator of relative peak intensity, $I_{1582/1071}$.

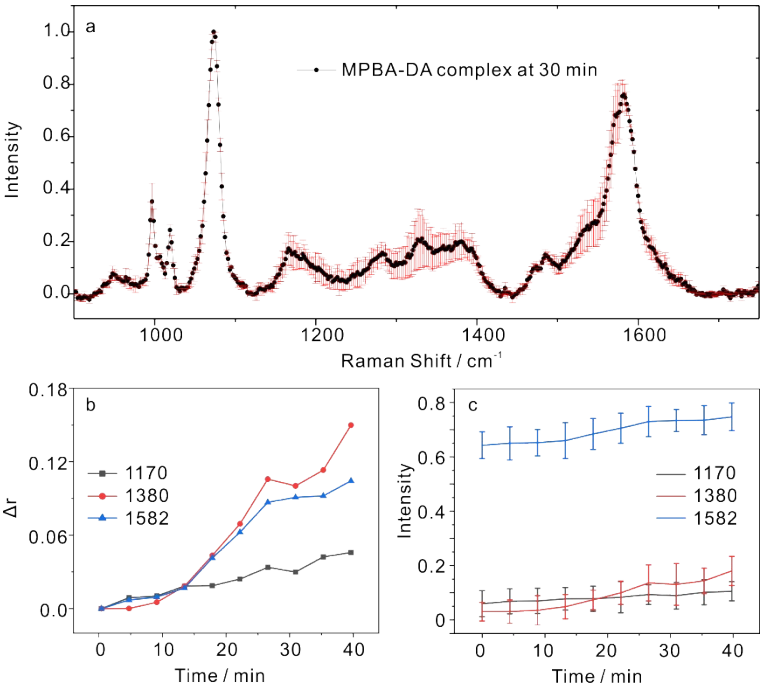

Figure S10. (a) Averaged SERS spectrum of MPBA-DA complexing at 30 min produced by triplicate measurements with standard deviations at each wavenumber. (b) Time-course variations (Δr) of $r_{1170/1071}$, $r_{1380/1071}$, and $r_{1582/1071}$ in Figure 2d. (d) Time-dependent values of $r_{1170/1071}$, $r_{1380/1071}$, and $r_{1582/1071}$ in Figure 2d.

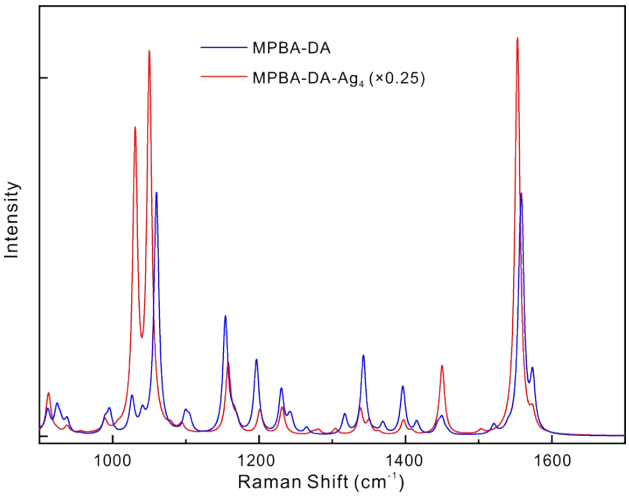

Figure S11. The Raman spectra of MPBA-DA and MPBA-DA bonded to an Ag_4 cluster.

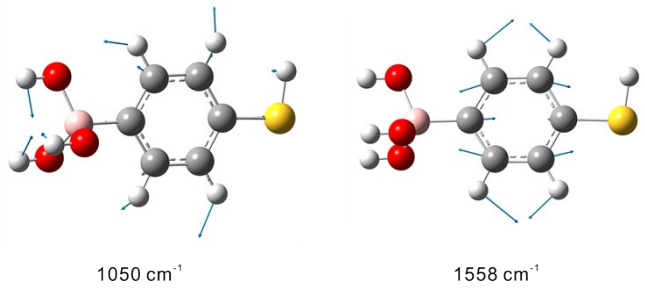

Figure S12. MPBA vibration mode at 1050 cm^{-1} and 1558 cm^{-1} in simulated Raman.

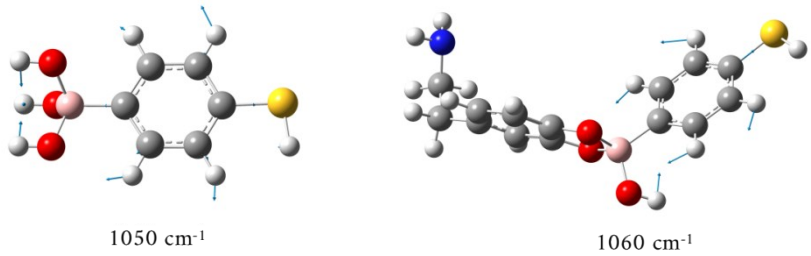

Figure S13. MPBA vibration mode at 1050 cm^{-1} and 1060 cm^{-1} in simulated Raman spectra of MPBA and MPBA-DA.

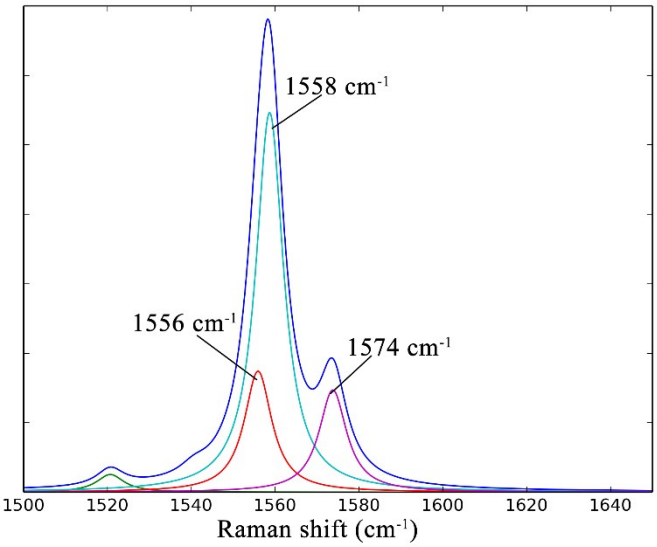

Figure S14. DFT calculated Raman spectrum of MPBA-DA and contributions of transition bands.